

Influence of Heat-Treatment Schedule on Glass-to-Metal Sealing Behavior

Yang Chong, Yang Dongliang, Zhang Yong, Chen Yongzhou, Shen Ziqin, Song Xiaozhen, Bao Sha

Beijing Key Laboratory of Fine Ceramics, State Key Laboratory of New Ceramics and Fine Processing, Tsinghua University, Beijing 100084, China

Abstract: The influence of heat-treatment schedule including sealing temperature and holding time on glass-to-metal sealing behavior in terms of average pore diameter and porosity was examined by optical microscopy. Results show that with the increasing sealing temperature, the average value of pore diameter firstly increases, then decreases, and at last increases. However, the porosity increases at first and becomes constant above 980 °C. Moreover, as the holding time prolonging, the average pore diameter increases gradually at first, and then decreases rapidly. While the porosity increases greatly, then increases slowly and decreases rapidly with increasing holding time. Additionally, the increases of both sealing temperature and holding time result in the increase of the thickness of bubble-free layer. A spatially varying bubble structure was presented by relating profiling to processing conditions.

Key words: glass; interfaces; microstructure; pores

Recently the technology of glass-to-metal sealing^[1] has been extensively used in many applications, such as electrical feed-through connectors^[2], solar cells^[3] and filtration devices^[4]. For these applications, the main motivation for developing a glass-metal joint is that it can lead to a higher level of hermeticity and reliability than a ceramic-metal joint^[5]. In the case of nuclear reactor application, glass-metal joints are necessary for the fixation of the metal conductor to a metal structure to perform diagnostics. The gap between individual metal conductor pin and the external metal body has to be sealed properly and tightly in order to realize quality isolation, ideal electrical insulation and good mechanical characteristics.

In order to achieve a mechanically strong adherent and hermetic seal between glass and metals, specific requirements need to be carefully considered. These requirements include forming chemical bindings at the interface between glass and metals^[6]. Additionally, the thermal expansion properties of the components could be ideally matched in order to hold back the emergence of harmful stress in the seals when cooling

down after sealing. However, another typical technique, compressive sealing, requires the coefficients of thermal expansion of the components orderly to decrease from the outside to the inside.

There are a lot of factors which will influence the characteristics of glass-metal seals^[7]. The emergence of voids or bubbles at the glass-metal interface is especially troublesome and can not only mechanically weaken the interface, but may damage the hermeticity of the seals^[8]. Previous studies have shown that the bubbles resulting from many factors and different methods have been selected in order to reduce this effect. However, there have been few studies on the processing conditions dependence of bubbles evolution at interfaces of the glass and metals.

In the present study, the formation and migration mechanism of bubbles during compressive sealing was investigated. To begin this investigation, a kind of silicate borate glass was selected and optical microscopic images for the glass-to-metal seals under different sealing temperatures and holding time

Received date: December 10, 2018

Foundation item: Project of Beijing Municipal Science & Technology Commission

Corresponding author: Zhang Yong, Ph. D., Professor, Beijing Key Laboratory of Fine Ceramics, State Key Laboratory of New Ceramics and Fine Processing, Institute of Nuclear and New Energy Technology, Tsinghua University, Beijing 100084, P. R. China, Tel: 0086-10-80194055, E-mail: yzhang@tsinghua.edu.cn

Copyright © 2019, Northwest Institute for Nonferrous Metal Research. Published by Science Press. All rights reserved.

were observed. The sealing experiments were conducted at four different temperatures (960, 980, 1000, and 1020 °C) and for four different isothermal holding periods (5, 10, 20, and 30 min). The principal motivation of this study originated from the need of generating a more comprehensive understanding of the glass-to-metal sealing processes. A secondary objective was to deeply study the bubble migration process which will be used to reduce bubbles in the glass-metal seals.

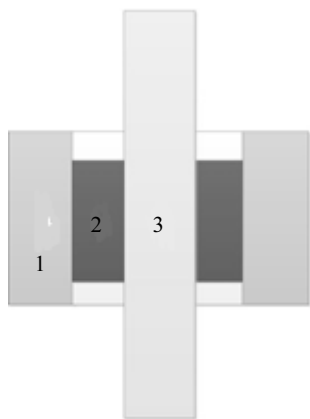
1 Experiment

A kind of glass with special composition of $15\text{BaO}-3\text{TiO}_2-10\text{CaO}-6\text{K}_2\text{O}-6\text{B}_2\text{O}_3-60\text{SiO}_2$ was used as a sealing glass with CTE (coefficient of thermal expansion) larger than that of metal pin and less than that of bulk head metal surrounding it, as shown in Fig.1. The glass was made from corresponding constituent oxides, which were well mixed and melted at 1550 °C for 3 h, and then quenched in the de-ionic water. The resulted glass slurry was dried and then attrition-milled for 7 h with ethanol as media. After drying, the resulted glass powder and a suitable amount of organic binder were well mixed and pressed into greenware tubes with 10 MPa pressure. The burnout of binder was followed and carried out at a temperature of 600 °C for 6 h. After that, sintering of the obtained glass tubes was performed at 650 °C for 60 min. The preparation procedure of the glass tubes has been given before^[9].

The outer diameter, inner diameter and length of the glass tubes used in the sealing experiment are 6.25, 2.6 and 9.5 mm, respectively.

Chemical composition of the alloy used as the metal pin is 87%Fe-12%Cr-0.028%Co. The diameter and length of the metal pin are 2.5 and 20 mm, respectively. Chemical composition of the stainless steel used as the metal bulkhead is 4%Mn-8%Ni-18%Cr-60%Fe. The outer diameter, inner diameter and length of metal body are 19.96, 6.3 and 9.5 mm, respectively.

Before being sealed, the sintered glass tubes, metal pin and



1-metal bulk head; 2-sealing glass; 3-metal pin; CET1>CET2>CET3

Fig.1 Schematic of compressive sealing

body were ultrasonically cleaned in alcohol for 10 min. Then, the components were rinsed with deionized water, dried and moved into an oven with a fixture for the sealing process.

The samples were heated to the sealing temperatures of 960, 980, 1000, and 1020 °C with a rate of 5 °C/min. For each sealing temperature, four different isothermal holding periods of 5, 10, 20, and 30 min were carried out. After the sealing experiment, the samples were cooled with a rate of 25 °C/min to 550 °C and kept for 70 min, and then cooled down to room temperature with a rate of 20 °C/min. Thermal treatments above were all conducted in a flowing nitrogen atmosphere.

The thermal expansion behaviors of the materials in the shape of a rod with 8 mm in diameter were measured with a heating rate of 5 °C/min by a dilatometer (Linseis L76/1250, Germany). $\alpha\text{-Al}_2\text{O}_3$ was selected as reference material. The measured CTEs of the components in the temperature range of 25~375 °C are 12×10^{-6} , 8×10^{-6} and 4.5×10^{-6} K⁻¹ for metal bulk head, sealing glass and metal pin, respectively.

The glass-metal sealing samples were trimmed and polished. Then the glass-to-metal interface was observed using an optical microscope (JVC TK-C9201EC). Image J was used to analyze the porosity and the pore diameter^[10]. Through making binary, the morphology was identified by grey value in the Image J program. Dark pores can be differentiated from the light condensed background. Each data of porosity and average value of pore diameter was achieved from six photos by calculating the average value.

2 Results and Discussion

Optical microscopy analyses of the glass-metal seals were carried out to better depict the sealing behavior. Fig.2 illustrates the sealing temperature influence on the glass parts. A typical image of the samples sealed at low sealing temperature is shown in Fig.2a, which shows that a lot of small pores appear. While Fig.2b shows the number of big pores increases with increasing sealing temperature. At the sealing temperature of 1000 °C, however, the number of big pore decreases and the number of small ones increases compared with Fig.2b. When the temperature increases to 1020 °C, more big pores emerge due to merging of small ones.

The dependence of average value of pore diameter as well as porosity on sealing temperature is shown in Fig.3. With the increase of sealing temperature, the average pore diameter firstly increases, then decreases and finally increases again. However, the porosity increases at first and becomes constant above 980 °C if the errors are taken into account. Considering that the porosity is related to both pore number and pore diameter, the pore number contribution to the porosity should be resolved. As shown in Fig.2, when the sealing temperature increases from 960 °C to 980 °C, both the pore number and pore diameter increase. Therefore, the porosity increases with the sealing temperature. But when the sealing temperature increases up to 1020 °C, the pore number seems to change in

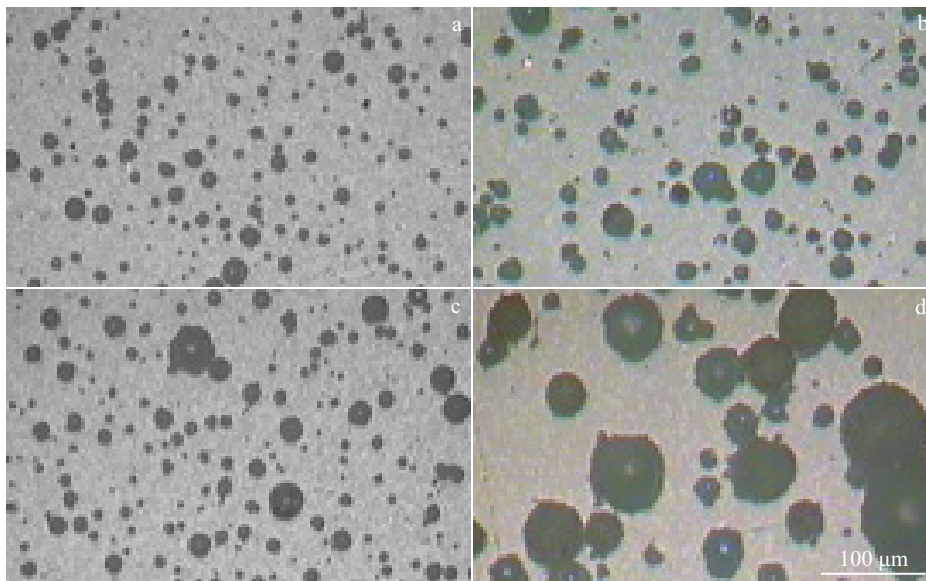


Fig.2 Optical microscopic images of the glass-metal sealing samples after heat treatment at different sealing temperatures for 10 min: (a) 960 °C, (b) 980 °C, (c)1000 °C, and (d) 1020 °C

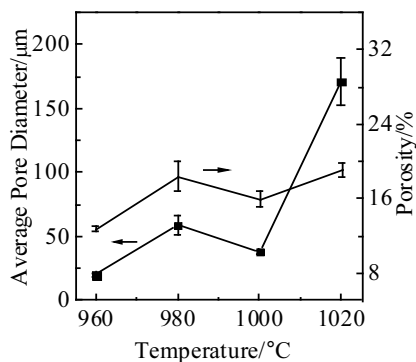
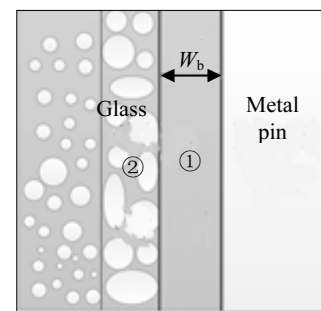


Fig.3 Variations of average pore diameter and porosity with increasing sealing temperature

the opposite direction, compared to pore diameter. This coupling makes the porosity keep constant.

One interesting point is that a bubble-free layer is observed at the interface of the glass and metal pin. Fig.4 shows a schematic illustration of two types of layer at the glass-metal interfaces, that is, bubble-free layer and bubble-rich layer. The sealing temperature dependence of the glass-metal interfaces is shown in Fig.5. It is obvious that the thickness of the bubble-free layer gradually increases with increasing the sealing temperature.

Fig.6 are optical images of the glass parts sealing at the temperature of 980 °C with various holding time. Fig.6a is a typical image of sample sealed with the holding time of 5 min. This image reveals big pores that coexist with small pores. The pore diameter becomes larger with prolonging holding time



①- bubble-free layer; ②- bubble-rich layer

Fig.4 Schematic of the interface between glass and metal pin

to 10 min. At 20 min, the number of pores increases, as shown in Fig.6c. But further prolonging results in a decrease in the number of pores.

Fig.7 precisely shows the change of average value of pore diameter as well as porosity as functions of holding time. It reveals that the average value of pore diameter increases first when the holding time increases from 5 min to 10 min and then decreases with longer holding time, whereas the average value of pore diameter is maximum at the holding time of 10 min. Different trends are shown for porosity with holding time. The porosity increases greatly between 5 min and 10 min, then increases slowly between 10 min and 20 min, and finally decreases rapidly between 20 min and 30 min.

The change of the thickness of bubble-free layer with the variation of holding time was observed again. Fig.8 are optical images which show the holding time dependence of W_b at the

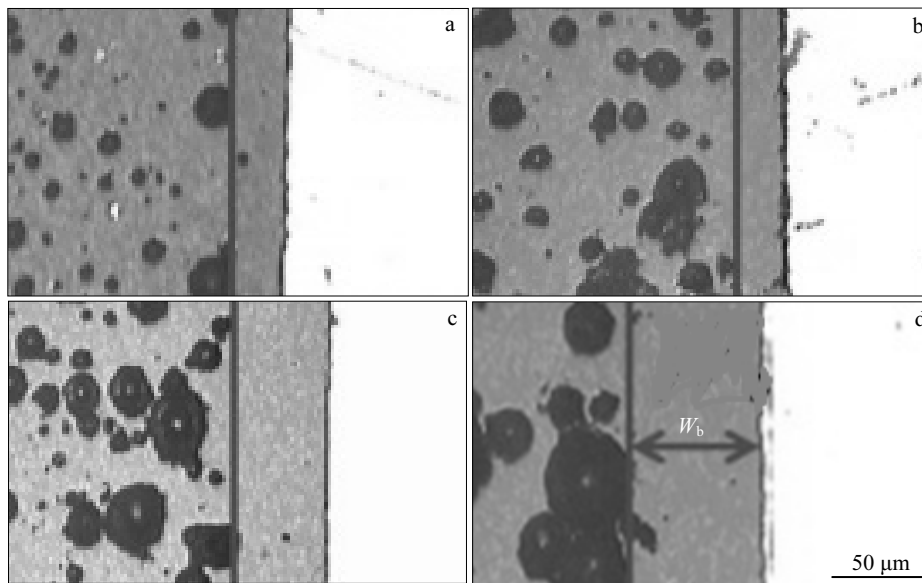


Fig.5 Optical microscopic images of the bubble-free layer with different sealing temperatures: (a) 960 °C, (b) 980 °C, (c) 1000 °C, and (d) 1020 °C

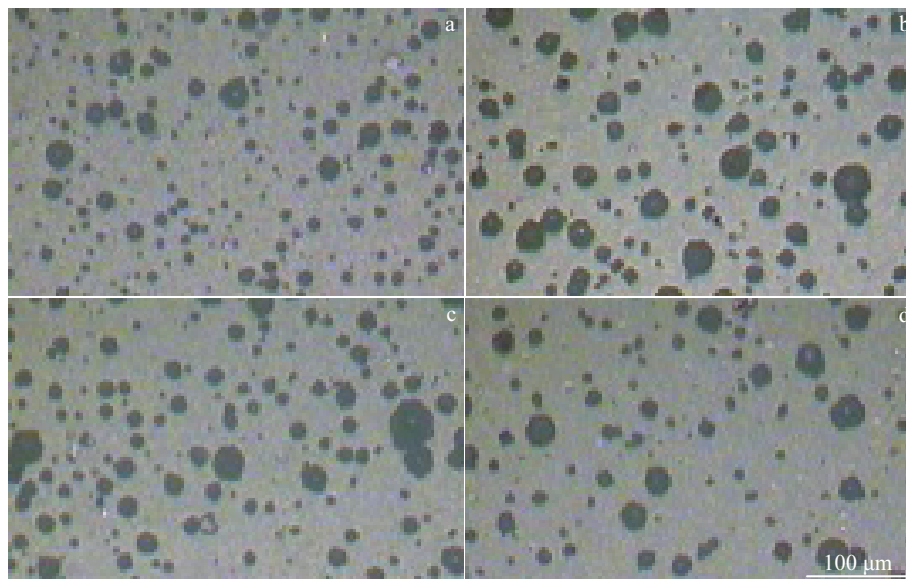


Fig.6 Optical microscopic images of the glass-metal sealing samples after heat treatment at 980 °C for different time: (a) 5 min, (b) 10 min, (c) 20 min, and (d) 30 min

glass-metal interfaces. It was observed that the value of W_b at the glass-metal interface systematically increases as the holding time increases.

An important feature in Fig.7 is the irregular trend of the average pore diameter and the porosity between 10 min and 20 min. When the decreasing trend of the average pore diameter was compared with the increasing one of the porosity, it is evident that the number of pores increases, as shown in Fig.6. When the holding time increases (up to 30 min), both the average pore diameter and the porosity are reduced further, demon-

strating that more bubbles escape from the melt. Prolonging holding time at 980 °C results in an increase of W_b , in agreement with the above-mentioned sealing temperature studies.

The mechanism implies those results above can be illustrated in terms of pore evolution which occurs by bubble nucleation, growth, and escape during the sealing process^[11], where the liquid phase flow promotes the collision, coalescence and movement of bubbles, resulting in corresponding variation of porosity distribution. On the one hand, the viscosity which decreases with increasing temperature^[12]

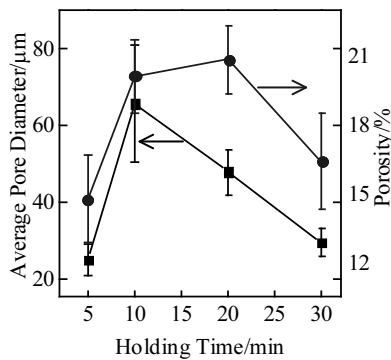


Fig.7 Variations of average pore diameter and porosity with increasing holding time

plays an important role in pore evolution. V is the rising velocity of bubbles in the molten glass and can be approximated via the following equation^[13]:

$$V = \rho g D^2 / k \eta \tag{1}$$

where, g is the gravitational constant, ρ is the density of the melt, D is bubble diameter, the factor k indicates a departure from the formula above and η represents the glass viscosity. With increasing temperature to some degree, much bigger pores under the influence of buoyancy are easier to escape from the melt. On the other hand, the pressure also plays a role in the pore evolution. When the internal gas pressure, P_{gas} , is large enough to exceed the outer forces, the pore will escape from the melt. The outer forces are from the ambient pressure, P_A , and the pressure in the bubble, P_C , which originates from the interfacial energy of the bubble-melt. The expression for pore growth in the melt is given by

$$P_{gas} \geq P_A + P_C \tag{2}$$

where, $P_C = 2\sigma/r$, σ is the surface tension of the melt; r is the

radius of the bubble^[14].

Based upon the analysis above, as shown in Fig.2 and 3, both average pore diameter and porosity do not decrease until a sealing temperature of 980 °C. It is supposed that both the low viscosity and high internal gas pressure contribute to the bubble growth and escape. In the range of 1000 °C to 1020 °C, it is the lower viscosity and bigger internal gas pressure that result in bubble escaping from the melt. The variation of average pore diameter with sealing temperature seems to be a good indication of the pore evolution in the sealing process.

By following the procedure described above for sealing at 980 °C, bubble evolution with various holding time can be extracted from observed pictures. As shown in Fig.6 and 7, prolonging holding time modifies the bubbles evolution characteristic of glass-metal interface. This implies that variations in average pore diameter and porosity occur due to the prolongation of holding time. It appears that average value of pore diameter is strongly reduced by prolonging holding time, and the value of porosity slightly decreases. The holding time dependence of the bubble evolution is due to the viscosity and internal gas pressure which have great effect on the bubbles movement, growth and escape according to Eqs. (1) and (2).

Moreover, in Fig.5 and Fig.8, a consistent increasing trend has been presented to explain microscopic observations on the thickness of bubble-free layer with various sealing temperatures and holding time. Increases of both sealing temperature and holding time will change the viscosity and internal gas pressure and eventually result in the movement of bubbles and the increase of the thickness of bubble-free layer.

Furthermore, a spatially varying bubble model can be constructed to obtain a complete understanding of pore evolution by stacking layers with different temperatures on top of one another, each with a different value of thickness. It is

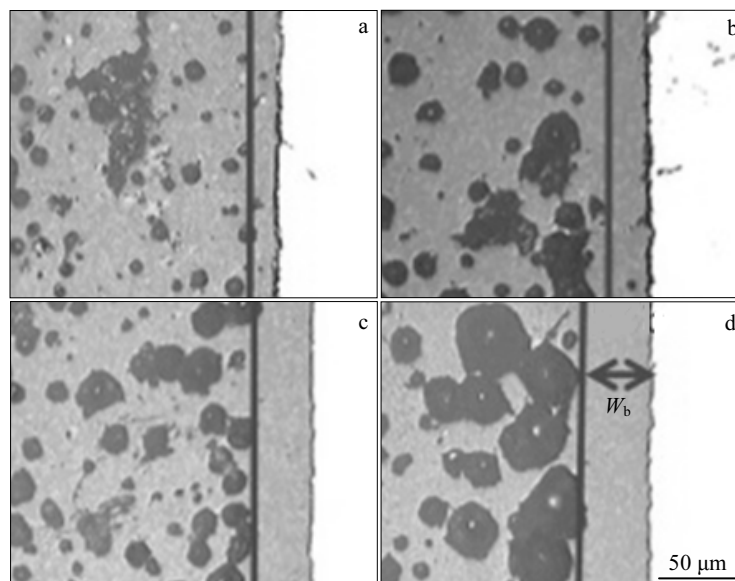


Fig.8 Optical microscopic images of the bubble-free layer with different holding time: (a) 5 min, (b) 10 min, (c) 20 min, and (d) 30 min

believed that differences in temperature, which have influences on surface tension, produce a displacive force upon the bubbles^[15] which could move in a temperature gradient. Even bigger ones will drag smaller bubbles to move^[16]. During the cooling stage, due to the higher thermal conductivity, the temperature of the metal pin decreases more rapidly than that of the sealing glass; therefore temperature gradient forms from the pin to the glass tube. The bubbles are supposed to move away from the metal pin, around which the temperature is lower and the viscosity of the glass is higher. Once the moving bubbles coalesces with the small bubbles, a bubble-rich layer will form and the remaining layer is bubble-free. And the bigger the pore diameter is, the larger the thickness of the pore-free layer remains. Thus, it is concluded that the bubble distribution structure for the case of a spatially varying bubble model is a representative physical picture.

3 Conclusions

1) When the sealing temperature increases, the average value of pore diameter firstly increases, then decreases, and at last increases. However, the porosity increases at first and becomes constant above 980 °C. In addition, the average value of pore diameter increases gradually at first, and then decreases rapidly with increasing holding time. Different trends are shown for the porosity with holding time, the porosity increases greatly, then increases slowly and decreases rapidly.

2) Increasing sealing temperature or prolonging holding time leads to an increase in the thickness of bubble-free layer. Pore evolution during the sealing process has been discussed. The variations of both viscosity and internal gas pressure are believed to be the main reason. A spatially varying bubble model was presented by relating profiling to processing conditions. The results of this work will provide some guidance on the manufacturing processes of glass-to-metal

sealing, since the occurrence of voids or bubbles at the glass-metal interface is particularly troublesome and cannot only mechanically weaken the interface, but may also prevent a seal from being hermetic.

References

- 1 Donald I W. *Journal of Materials Science*[J], 1993, 28(11): 2841
- 2 Staff M T, Fernie J A, Mallinson P M et al. *International Journal of Applied Ceramic Technology*[J], 2016, 13(5): 956
- 3 Selcuk A, Atkinson A. *Fuel Cells*[J], 2015, 15(4): 595
- 4 Xiao Z H, Sun X Y, Liu K et al. *Journal of Alloys and Compounds*[J], 2016, 657: 231
- 5 Intrater J. *Materials and Manufacturing Processes*[J], 1993, 8(3): 353
- 6 Luo D W, Shen Z S. *Journal of Alloys and Compounds*[J], 2009, 477(1-2): 407
- 7 Lin C K, Liu Y A, Wu S H et al. *Journal of Power Sources*[J], 2015, 280: 272
- 8 Donald I W, Metcalfe B L, Gerrard L A. *Journal of the American Ceramic Society*[J], 2008, 91(3): 715
- 9 Yang D L, Zhang Y, Song X Z et al. *Ceramics International*[J], 2016, 42(5): 5906
- 10 Schindelin J, Arganda-Carreras I, Frise E et al. *Nature Methods*[J], 2012, 9: 676
- 11 Martel C, Bureau H. *Earth and Planetary Science Letters*[J], 2001, 191(1-2): 115
- 12 Axinte E. *Materials & Design*[J], 2011, 32(4): 1717
- 13 Ellison A, Cornejo I A. *International Journal of Applied Ceramic Technology*[J], 2010, 1(1): 87
- 14 Yang C C, Nakae H. *Journal of Materials Processing Technology* [J], 2003, 141(2): 202
- 15 Wilcox W R, Suhrmanian R S, Papazian J M et al. *AIAA Journal*[J], 1979, 17(9): 1022
- 16 Mattox D M, Smith H D, Wilcox W R et al. *Journal of the American Ceramic Society*[J], 1982, 65(9): 437

热处理制度对玻璃金属封接行为的影响

杨 冲, 杨冬亮, 张 勇, 陈永洲, 沈子钦, 宋晓贞, 包 莎

(清华大学 新型陶瓷与精细工艺国家重点实验室 精细陶瓷北京市重点实验室, 北京 100084)

摘 要: 借助光学显微镜观测手段, 通过分析玻璃金属封接过程中平均孔径和孔隙率随封接温度和保温时间的变化, 详细研究了热处理制度包括封接温度和保温时间对玻璃金属封接行为的影响。随着封接温度的升高, 平均孔径先增大后减小最后又上升, 然而孔隙率先出现增加趋势, 当封接温度高于 980 °C 时基本保持不变。随着封接时间的延长, 平均孔径先逐渐增加后迅速降低, 孔隙率则显著增加然后缓慢增加, 接着迅速降低。另外, 封接温度的提高和保温时间的延长都将导致无气泡带的变宽。根据封接热处理制度的变化, 提出了一种空间气泡演变结构模型。

关键词: 玻璃; 界面; 微观结构; 孔隙

作者简介: 杨 冲, 女, 1991 年生, 硕士, 清华大学核能与新能源技术研究院, 新型陶瓷与精细工艺国家重点实验室, 精细陶瓷北京市重点实验室, 北京 100084, 电话: 010-80194055, E-mail: 767522921@qq.com